Fate of ZnO nanoparticles in soils and cowpea (Vigna unguiculata)

Journal:	*Environmental Science & Technology*
Manuscript ID:	es-2013-03466p.R2
Manuscript Type:	Article
Date Submitted by the Author:	26-Oct-2013
Complete List of Authors:	Wang, Peng; The University of Queensland, School of Agriculture and Food Sciences Menzies, Neal; The University of Queensland, Lombi, Enzo; University of South Australia, Centre for Environmental Risk Assessment and Remediation McKenna, Brigid; The University of Queensland, Johannessen, Bernt; Australian Synchrotron, Glover, Chris; Australian Synchrotron, Kappen, Peter; Australian Synchrotron, Kopittke, Peter; The University of Queensland, ; The University of Queensland,

Fate of ZnO nanoparticles in soils and cowpea (*Vigna unguiculata*)

Peng Wang,[†,] Neal W. Menzies,[†] Enzo Lombi,[‡] Brigid A. McKenna,[†] Bernt Johannessen,[§] Chris J. Glover,[§] Peter Kappen,[§] and Peter M. Kopittke[†]*

[†]School of Agriculture and Food Sciences, The University of Queensland, St. Lucia, Queensland, 4072, Australia

[‡]Centre for Environmental Risk Assessment and Remediation, University of South Australia, Mawson Lakes, South Australia, 5095, Australia

[§]Australian Synchrotron, Clayton, Victoria, 3168, Australia

[*]To whom correspondence should be addressed. Phone: +61 7 3365 4816, Fax: +61 7 3365 1177, Email: p.wang3@uq.edu.au

Abstract

The increasing use of zinc oxide nanoparticles (ZnO-NPs) in various commercial products is prompting detailed investigation regarding the fate of these materials in the environment. There is, however, a lack of information comparing the transformation of ZnO-NPs with soluble Zn^{2+} in both soils and plants. Synchrotron-based techniques were used to examine the uptake and transformation of Zn in various tissues of cowpea (*Vigna unguiculata* (L.) Walp.) exposed to ZnO-NPs or $ZnCl_2$ following growth in either solution or soil culture. In solution culture, soluble Zn ($ZnCl_2$) was more toxic than the ZnO-NPs, although there was substantial accumulation of ZnO-NPs on the root surface. When grown in soil, however, there was no significant difference in plant growth and accumulation or speciation of Zn between soluble Zn and ZnO-NP treatments, indicating that the added ZnO-NPs underwent rapid dissolution following their entry into the soil. This was confirmed by an incubation experiment with two soils, in which ZnO-NPs could not be detected after incubation for 1 h. The speciation of Zn was similar in shoot tissues for both soluble Zn and ZnO-NPs treatments and no upward translocation of ZnO-NPs from roots to shoots was observed in either solution or soil culture. Under the current experimental conditions, the similarity in uptake and toxicity of Zn from ZnO-NPs and soluble Zn in soils indicates that the ZnO-NPs used in this study did not constitute nano-specific risks.

Keywords: ZnO nanoparticles, uptake, toxicity, transformation, soil, plant, zinc

INTRODUCTION

Engineered nanoparticles (ENPs) are being developed and incorporated into a variety of industrial, commercial, and medicinal products. Zinc oxide nanoparticles (ZnO-NPs) are among the most commonly used ENPs in personal care products (e.g. sunscreens, cosmetics), textiles, paintings, industrial coatings, dye-sensitized solar cells, antibacterial agents, and optic and electronic materials.[1] In addition, ZnO-NPs have been proposed as an effective Zn fertilizer to alleviate Zn deficiency in soils.[2] While some of these commercial applications, and their relative exposure pathways (e.g. through the wastewater treatment process), are unlikely to lead to the direct release of ZnO-NPs to the environment, others (e.g. fertilisers) could lead to their direct release to the soil. As a novel and emerging class of products, the ecological risk of ZnO-NPs is an important topic that is receiving increased scrutiny from both the scientific and regulatory viewpoints.

Plants are an important component of the ecological system and serve as a potential pathway for the transportation and accumulation of ENPs into the food chain.[3-5] There is evidence that particles up to 20 nm are taken up by plant cells through plasmodesmata and endocytosis.[6] Indeed, some studies have demonstrated the uptake of ENPs by plants grown in solution culture. For example , Lin and Xing[7] used transmission electron microscopy (TEM) to show that ZnO-NPs passed through the epidermis and cortex of roots of *Lolium perenne* L. (ryegrass), but did not examine if they are present within the shoots. Zhu et al.[3] used magnetization to show the uptake and subsequent transport of magnetite Fe_3O_4-NPs by *Cucurbita maxima* (pumpkin) grown in solution culture. However, no Fe_3O_4-NPs (i.e. magnetic signals) were detected in shoots of soil-cultured plants. This is similar to other soil- or sand-based studies, which were unable to detect plant uptake of NPs. For example, no ZnO-NPs were detected in either roots [8] or shoots [9] of wheat (*Triticum aestivum* L.) or in stems and pods of soybean (*Glycine max* (L.) Merr.) [10], and no CeO_2 NPs were detected in leaves of maize (*Zea mays* L.).[11] These findings suggest that the growth matrix affects the uptake of NPs, but, to our knowledge, there are no data quantifying the differences in the uptake and transformation (i.e. the chemical form) of ZnO-NPs in various tissues of plants grown in different growth matrices.

The absence of ZnO-NPs in shoots may be explained by their attachment to the soil particles or the rapid dissolution and transformation of ZnO-NPs upon entering the soil. Indeed, it has been suggested that ZnO-NPs undergo quick dissolution/transformation upon their release into the environment.[12-15] Although most ZnO-NPs released from consumer products are likely converted to other species before entering the soil as applied biosolids,[13] the application of ZnO-NPs as a Zn fertilizer (including as a foliar fertilizer) has also been proposed.[2] Indeed, there is growing interest in the use of ZnO-NPs as fertilizers as Zn deficiency is by far the most widespread micronutrient deficiency limiting crop production in the world.[16] In the case of soils, however, little is known about the fate of ZnO-NPs over time.

The aims of this study were (i) to compare the uptake and toxicity (and subsequent transformation) of ZnO-NPs and $ZnCl_2$ to inform the associated environmental risks, and (ii) to determine if there are any differences between the uptake of the Zn in soil or solution culture. In this study, we examined the speciation of Zn within various tissues of plants exposed to ZnO-NPs or $ZnCl_2$ in solution or soil culture and assessed the fate of ZnO-NPs over time in two soils (differing in chemical and physical properties).

MATERIALS AND METHODS

Zinc Oxide Nanoparticles. The ZnO-NP dispersion, synthesized by the hydrolysis of a zinc salt in a polyol medium heated to 160 °C, was purchased from Sigma Aldrich (catalog No. 721077). This product has a reported particle size < 100 nm measured by dynamic light scatting (DLS) and an average particle size < 35 nm measured using an aerodynamic particle sizer (APS) spectrometer. Our analyses of the suspensions used for the experiments by DLS using a Zetasizer Nano (Malvern Instruments, Worcestershire, UK) gave an average number-weighted particle size of 67 ± 2 nm and zeta potential of +46.1 ± 1.5 mV. Images analysed by field emission scanning electron microscopy (SEM, JEOL JSM 6400 F) indicated a crystallite size range of 20−30 nm.

Plant Growth Conditions. Both solution and soil culture experiments were conducted simultaneously in a semi-controlled glasshouse in full sunlight at The University of Queensland, St Lucia, Australia. The temperature was maintained at ca. 28°C during the day and 20°C during the night. Relative humidity typically ranged between 25 and 50% during the day and 60 to 80% during the night.

Solution Culture. Seeds of cowpea (*Vigna unguiculata* (L.) Walp. cv. Red Caloona) were germinated in trays covered with paper towel moistened with tap water. After 2 d, seedlings were transferred to containers with 11 L of nutrient solution (μM): 800 NO_3^--N, 120 NH_4^+-N, 650 Ca, 100 Mg, 300 K, 550 SO_4^{2-}-S, 140 Cl, 10 P, 10 Fe (supplied as Fe(III)CDTA), 3.0 B, 1.0 Mn, 0.05 Cu, 0.01 Zn, and 0.02 Mo. Solution pH was not adjusted but averaged pH 6.1. After a further 3 d, four seedlings were transferred to four replications of 11 L solutions (as above) containing no added Zn (control) or with Zn added as either ZnO-NPs or $ZnCl_2$ to achieve a final concentration of 25 mg Zn L^{-1} (38.2 μM). This Zn concentration has been shown to reduce root growth by approximately 70% [17] and is within the range found in soil solutions.[18] Solutions were continuously aerated and renewed every 4 d, with plants harvested after 4 weeks. At harvest, the roots were washed with flowing deionized water for ca. 1 min and blotted dry with filter paper, before the roots, stems, and leaves were separated. Subsamples of each tissue were immersed in liquid nitrogen and immediately stored in a dry shipper cooled with liquid nitrogen for later analysis using X-ray absorption spectroscopy (XAS). The remaining tissues were oven-dried for analysis using inductively coupled plasma mass spectrometry (ICP-MS) (details provided below).

Soil Culture. An Oxisol (US Soil Taxonomy) with pH 6.7 and a sandy clay texture, collected from a site near Toowoomba, Queensland (Table S1), was air-dried and sieved to < 2 mm. The soil was amended with either ZnO-NPs or $ZnCl_2$ with a target concentration of 500 mg Zn kg^{-1} soil as used by Priester et al.[19] This concentration is far in excess of that expected under a fertilisation scenario and could only be conceived to result from an unintentional spill of concentrated ZnO-NP solutions. However, this is the highest concentration used by Priester et al.[19] reporting a negative impact of ENPs on soil fertility and soybean growth. As pointed out by Lombi et al.[20], the above-mentioned article did not include a soluble

Zn treatment and it was therefore not possible to draw any definitive conclusion regarding any nano-specific effects with regard to toxicity. In this article, we provide such comparison which is essential in the context of the debate regarding the environmental consequence of nanotechnologies. To ensure even distribution of Zn in the soil, the ZnO-NP suspensions or $ZnCl_2$ solutions (20 mg Zn mL^{-1}) were diluted with deionized water to a volume of 50 mL and sprayed over 2 kg dry soil which was then mixed thoroughly by hand. A control (no added Zn) was also included by spraying with the same volume of deionized water. Each treatment was replicated three times with 2.0 kg soil in each 4 L plastic pot. Soils were watered to 60% of water holding capacity and equilibrated for 1 d prior to planting. Six 3-d old seedlings were transferred to each pot and three seedlings harvested after 4 weeks. The shoots were rinsed with deionized water and separated into stems and leaves. The root system was removed by carefully breaking apart the soil and then rinsing with deionized water for ca. 1 min, blotted dry, and separated into roots and nodules. Samples of each tissue were immersed in liquid nitrogen and stored in a dry shipper for later analysis using XAS. The remaining samples were oven-dried for analysis using ICP-MS. The remaining three plants in each pot were harvested at maturity (ca. 80 d after planting) and samples of seeds ground to fine powder for later analysis using XAS and ICP-MS.

Soil Incubation Experiment. The fate of ZnO-NPs following addition to soil was investigated in the Oxisol (described above) and in an Ultisol (US Soil Taxonomy) collected from the Central Highlands of Queensland. This soil is an acidic (pH 5.0) sandy loam soil (Table S1). Two replicates (100 g) of both soils were amended with ZnO-NPs or $ZnCl_2$ to a target concentration of 500 mg kg^{-1} soil as described above, placed in 300 mL beakers, and deionized water added to 60% of soil water holding capacity. Each beaker was covered and sealed with plastic film with small holes to maintain relatively constant moisture; deionized water was added every 4 d if necessary. Soils were incubated in the dark at 25 ± 2°C, and samples collected after 1 h, 1 d, 5 d, and 15 d, immediately frozen (ca. -20°C), and later freeze-dried for analysis using XAS.

Bulk XAS. Zinc K_α-edge X-ray absorption near edge structure (XANES) and extended X-ray absorption fine structure (EXAFS) spectra were collected at the XAS Beamline at the Australian Synchrotron, Melbourne as described by Kopittke et al.[21] The energy of each spectrum was calibrated by simultaneous measurement in transmission mode of a metallic Zn foil reference (K_α-edge at 9,659 eV). The spectra were collected in fluorescence mode with a 100-element solid-state Ge detector. To prepare samples, ca. 1-2 g frozen plant tissues were homogenized in an agate mortar and pestle continuously cooled with liquid nitrogen.[17] Soil and seed samples were ground using a mortar and pestle and sieved to < 250 µm using a stainless steel sieve. A total of 29 Zn standards was also examined, including six aqueous compounds [21] and 23 finely ground powder spectra [13]. The aqueous standards were used for fitting Zn ligands in plant tissues and the solid standards for Zn ligands in soils. Due to the low concentration of Zn in some fresh plant samples, only XANES spectra were collected for plant samples, while both XANES and EXAFS spectra were collected for soil samples. The spectra (average of three scans) were energy normalized using Athena software.[22] Principal component analysis (PCA) of the normalized sample spectra was used to estimate the likely number of species contained in the samples, while target transformation (TT) was used to identify relevant standards for linear combination fitting (LCF) of the sample spectra.[23] PCA and TT were undertaken using SixPack.[24] For both XANES (-20 to +30 E, eV) and EXAFS (2.5 to 9 k, $Å^{-1}$), LCF was performed using Athena.

X-ray Fluorescence Microscopy (µ-XRF). Elemental µ-XRF maps were collected at the XFM Beamline at the Australian Synchrotron [25] using roots exposed to 25 mg Zn L^{-1} as ZnO-NPs or $ZnCl_2$ for 1 d. In addition, mature seeds of plants grown in the Oxisol amended with ZnO-NPs or $ZnCl_2$ were longitudinally sliced (ca. 200 µm) for µ-XRF analysis. The XRF spectra were analyzed using GeoPIXE [26] and the images were generated using the Dynamic Analysis method.[27]

Digestion and Analysis of Total Zn. Dry plant tissues were placed into 50 mL conical flasks and digested using 10 mL 5:1 HNO_3:$HClO_4$. Following digestion, the samples were diluted to 10 mL using deionized water before analysis by ICP-MS. Soil samples were digested with aqua regia (1:3 HCl:HNO_3)

and analyzed for total Zn by ICP-MS. Quality control measures included the use of procedural blanks and repeat analysis of a certified reference.

Statistical Analysis. Treatment-differences were tested for significance ($p < 0.05$) using a one-way analysis of variance (ANOVA) performed with IBM SPSS Statistics 20.

RESULTS

ZnO-NPs and Soluble Zn Effects on Plants. In solution culture, the addition of Zn reduced plant growth compared to that in the control (basal nutrient solution), with toxicity more severe in $ZnCl_2$ solutions than with those containing ZnO-NPs (Table S2). In contrast, there were no significant effects ($p > 0.05$) on plant growth between the control and the ZnO-NP and $ZnCl_2$ treatments in soil culture.

After 4 weeks in solution culture, Zn concentration in roots exposed to ZnO-NPs (44,700 μg g^{-1} dry mass, DM) was 4.6-times higher than those exposed to $ZnCl_2$ (9,650 μg g^{-1} DM). Concentrations in stems (487 and 584 μg g^{-1} DM) and leaves (119 and 139 μg g^{-1} DM) were similar between the ZnO-NP and $ZnCl_2$ treatments (Table S3). As a consequence, the Zn transfer coefficient (i.e. the ratio of Zn in the leaf relative to the root) was 4.7-times lower in the ZnO-NP treatment (0.003) compared to that in the $ZnCl_2$ treatment (0.014). This similarity indicated that the increased accumulation of Zn in roots exposed to ZnO-NPs in solution culture is likely due to either an increased adhesion or limited transport of ZnO-NPs to the shoot. In the case of soil culture, there were no significant differences ($p > 0.05$) in Zn concentrations of roots (1,003 and 1,180 μg g^{-1} DM), stems (108 and 118 μg g^{-1} DM), leaves (155 and 181 μg g^{-1} DM), or seeds (43.3 and 55.7 μg g^{-1} DM) between the ZnO-NP and $ZnCl_2$ treatments (Table S3). Transfer coefficients in soil culture (0.155 and 0.154) were substantially higher than those in solution culture.

Zinc Speciation and Distribution in Plant Tissues. The Zn XANES spectrum for ZnO-NPs (Figure 1) is readily identified due to its unique features, particularly the shoulder at 9,780 eV, and is similar to

previously-reported spectra for this material.[13, 14] The Zn XANES spectra for all other standards, while different from each other, were substantially different from that of ZnO-NPs.

Overall, it was apparent that the XANES spectra of roots exposed to ZnO-NPs in solution culture were markedly different from that obtained for the $ZnCl_2$-exposed roots, with the spectrum for ZnO-NP-exposed roots resembling that of the ZnO-NPs themselves (Figure 1A). It would appear that ZnO-NPs were the primary form of Zn in these samples – this being supported by the distribution of Zn using μ-XRF. Zinc was largely located on the root surface, most likely due to the adhesion and aggregation of ZnO-NPs (Figure 2A). Indeed, LCF revealed that ca. 65% of the Zn in these ZnO-NP-exposed roots was present as ZnO-NPs, with 32% associated with histidine (Table 1). In contrast, roots exposed to $ZnCl_2$ in solution culture accumulated Zn in the root apex (i.e. meristematic zone) (Figure 2A). This Zn was found to be associated with histidine (49%) and polygalacturonic acid (Zn-PGA, 32%), and Zn-phosphate (19%).

Interestingly, and in contrast to the solution culture results, the XANES spectra of roots grown in soil were similar regardless of whether the roots were exposed ZnO-NPs or $ZnCl_2$ (Figure 1B). Using LCF, the Zn in roots from these ZnO-NP and $ZnCl_2$ treatments was found to be associated with citrate (average 51%), histidine (28%), and phytate (20%) (Table 1). Given the similar concentration of Zn in roots exposed to ZnO-NPs and $ZnCl_2$ (Table S3), it is possible that the ZnO-NPs underwent dissolution in the soil.

The XANES spectra obtained for the stems and leaves from the ZnO-NP and $ZnCl_2$ treatments in both solution and soil culture were visually similar to the spectrum of Zn citrate (Figure 1). This observation was confirmed by LCF, with the Zn in these tissues mainly associated with citrate (50%), histidine (26%), and phytate (24%) (Table 1). In the root nodules, Zn was associated with citrate (37%), phytate (38%), and cysteine (27%) (Table 1).

The XANES spectra for seeds of plants grown in the ZnO-NP and $ZnCl_2$ treatments in soil showed a characteristic broader double-peaked feature, which resembled the Zn phytate spectrum in some regards (Figure 1B). However, the best fits using LCF included association with three components, histidine (50%), cysteine (30%) and phosphate (20%) (Table 1). Even if Zn phytate was included as one of the standards in the LCF, only 16-33% was calculated to be presented as Zn phytate, with the remainder of Zn present associated with cysteine (40-47%) and histidine (26-37%) (the R-factors increasing by 50 to 100% compared to the best fits). Therefore, ca. 70 to 80% of the Zn in the seeds was associated with amino acids (i.e. histidine and cysteine), with 20 to 30% bound to phosphate such as $Zn_3(PO_4)_2$ or as Zn phytate. The spatial distribution of Zn within the seeds determined using μ-XRF was found to be similar in the ZnO-NP and $ZnCl_2$ treatments. A high concentration of Zn was evident in the outer layer of cotyledon and the hypocotyl, with low Zn concentration in the seed coat (testa) and the inner cotyledon (Figure 2B).

Zinc Speciation in Soils.

Across the incubation periods examined, both XANES and EXAFS spectra were similar regardless of whether the soils were amended with $ZnCl_2$ or ZnO-NPs (Figure 3 and Table 2), indicating a rapid dissolution of the ZnO-NPs and that incubation for up to 15 d did not substantially change the speciation of Zn in either soil. In the Oxisol with $ZnCl_2$, LCF using the XANES spectra indicated that the Zn was present as Zn sorbed ferrihydrite (54%), ZnAl-layered double hydroxide (ZnAl-LDH) (22%), and $ZnSO_4$ (23%). In the case of the Ultisol, 35% of the Zn was calculated to be in a form resembling hopeite ($Zn_3(PO_4)_2$), with Zn also present as ZnAl-LDH (14%), Zn-humic acid (21%), and $ZnSO_4$ (30%) (Figure 3 and Table 2). These results regarding the presence of ZnAl-LDH and $ZnSO_4$ were reinforced by analysis of the EXAFS spectra (Table 2). Indeed, for both soils, LCF of the EXAFS spectra indicated that the Zn was present as 43% of hemimorphite ($Zn_4Si_2O_7(OH)_2 \cdot H_2O$), 29% as ZnAl-LDH, and 28% as $ZnSO_4$ (Table 2). The slight discrepancy between XANES and EXAFS LCF results has been reported previously[28, 29] and could be related to the lower sensitivity of EXAFS to metals bound to matrices composed of light elements or organic matter.[28]

Even when ZnO-NPs were added into the soil, almost all of the Zn was present in the same forms as when $ZnCl_2$ was added (Figure 3 and Table 2). The LCF of the XANES spectra for both soils revealed that no Zn could be detected in the form of ZnO-NPs after 1 h incubation. These results suggest that the large majority of the added ZnO-NPs underwent rapid dissolution following their entry into the soils. It should be noted, however, that changes in Zn speciation may have occurred during the time between the samples being transferred to −20 °C and their freezing.

DISCUSSION

In solution culture, soluble Zn ($ZnCl_2$) was more toxic than ZnO-NPs to the growth of cowpea (Table S2) despite the apparent accumulation of ZnO-NPs on the root surface (Figure 2 and Table S3). Interestingly, however, when grown in soil, there was no difference in plant growth between the $ZnCl_2$ and ZnO-NP treatments (Table S2). This difference between solution and soil culture highlights the importance of the growth matrix in plant culture experiments. Importantly, it was noted that there was also no significant difference in Zn concentration in shoots between the $ZnCl_2$ and ZnO-NPs treatments (Table S3) and we did not detected the upward translocation of ZnO-NPs from roots to shoots of plants grown in either solution or soil culture (Table 1 and Figure 1). Under the current experimental conditions, the ZnO-NPs added to the soil were rapidly converted to the same forms as when $ZnCl_2$ was added (Figure 3 and Table 2). This indicates that even at the high rate of ZnO-NPs added in the current study, no nano-specific effects (toxicity, uptake, speciation, and distribution) could be observed when plants were grown in soils. Thus, whilst Priester et al.[19] reported that the use of ZnO-NPs may result in “agriculturally associated human and environmental risks”, our data suggest that these risks for ZnO-NPs, under the current experimental conditions, would not different from those of soluble Zn. It is noteworthy that Priester et al.[19] did not include a soluble Zn control in their study.

In solution culture, accumulation of Zn in roots exposed to ZnO-NPs was 4.6-times higher than that in the $ZnCl_2$ treatment, but toxicity was more severe in solutions with $ZnCl_2$ (Tables S2 and S3). The majority

of the Zn in roots exposed to ZnO-NPs was on the root surface due to their adhesion and aggregation (Figure 2A). Indeed, the XAS analyses indicated that ca. 65% of Zn in these roots was present as ZnO-NPs (Table 1 and Figure 1). In addition, the speciation of Zn was similar in the shoots for both $ZnCl_2$ and ZnO-NP treatments and no ZnO-NPs were detected in shoot tissues despite the substantial accumulation of ZnO-NPs on the root surface (Table 1 and Figure 1). These observations indicate that the Zn uptake and toxicity was due to particle dissolution in the bulk nutrient solution and particle adhesion onto the root surface, rather than the uptake of nanoparticles. These findings are in accordance with previous reports[12, 30-32] which concluded that the toxicity of ZnO-NPs is due solely to solubilized Zn^{2+}.

In soil culture, there was no significant difference in plant growth or uptake of Zn between the two Zn treatments (Table S2 and S3). There was rapid equilibration through adsorption and precipitation reactions upon addition of soluble $ZnCl_2$ or ZnO-NPs to soil. This could be seen by the presence of ZnAl-LDH, hopeite, and hemimorphite (Table 2), the formation of which substantially reduced the toxicity of Zn to the plants. In addition, the phytotoxicity of Zn in soils depends on a range of soil properties (including pH and cation exchange capacity [CEC]). Indeed, Smolders et al.[33] reported that the EC10 (10% effective concentration) values for *Triticum aestivum* grown in a range of soils varied from 9 to 1,231 mg kg^{-1} (cf. 500 mg kg^{-1} used in pot experiment with a pH-neutral soil). The application of ZnO-NPs to the Oxisol (pH-neutral) and Ultisol (acidic) had similar effects to that of $ZnCl_2$ with no ZnO-NPs detected after incubating for 1 h (Table 2 and Figure 3). This finding suggests a rapid dissolution of ZnO-NPs in these soils, most likely driven by sorption of solubilized Zn^{2+} found in previous studies.[13, 14, 34-36] For example, Lombi et al.[13] found that ZnO-NPs in sewage sludge were converted to ZnS within 1 d. Similarly, Scheckel et al.[14] found that the addition of a clay mineral (kaolinite) resulted in the dissolution of ZnO-NPs within 1 d due to their sorption to the negative charge of the clay (78% of the ZnO-NPs sorbed within 1 h). Given that kaolinite has a similar (or lower) CEC (ca. 1-5 $cmol_c/kg$) relative to the soils used in the present study (2.3 or 13 $cmol_c/kg$, see Table S1), the observation that the ZnO-NPs underwent rapid dissolution upon their addition to the soils is in accordance with previous findings. However, it seems that the speed of dissolution of ZnO-NPs depends upon soil properties (particularly pH)

and the method used to add ZnO-NPs to the soil. For example, in contrast to the present study where ZnO-NPs could not be detected after 1 h in acidic soils, Collins et al.[36] found that dissolution of the ZnO-NPs required 30 d after sprinkling nanoparticles on the surface of an alkaline soil (pH 7.5). Similarly, using flow field-flow fractionation, Gimbert et al.[37] was still able to detect ZnO-NPs in suspensions of an alkaline soil (pH 9.0) spiked with 12,000 mg Zn kg^{-1} after 14 d incubation.

In the present study, no ZnO-NPs were detected in any shoot tissues regardless of growth matrix (Table 1 and Figure 1), indicating no transfer of ZnO-NPs from roots to shoots. This finding is in keeping with recent studies in which no ZnO-NPs could be detected in shoots of soil-grown soybean using XAS; rather, Zn was associated with citrate in the stem and seed pod[10]. Additionally, Zn phosphate was present in the shoots of wheat grown with added ZnO-NPs in sand culture.[9]

In roots exposed to $ZnCl_2$ in solution culture, the majority of the Zn was observed in the meristemic region (Figure 2A) and LCF analysis indicated that the Zn was primarily associated with histidine, with slightly smaller contributions from polygalacturonic acid (the main component of pectin in the cell wall) and precipitated as Zn-phosphate (Table 1). This suggests that histidine and the cell wall play important roles in Zn homeostasis and detoxification in roots. Similarly, Salt et al.[38] reported that the majority of the intracellular Zn in roots of *Thlaspi caerulescens*, a Zn hyperaccumulator, grown in solution culture was coordinated with histidine, with the remainder complexed to the cell wall. In the present study, however, no Zn was found to be present as Zn-phosphate within roots when grown in soil culture, but rather was associated with citrate, histidine, and phytate (Table 1). Zinc-phosphate precipitates have been observed at the surface of roots grown in solution culture[39, 40], being most likely related to the low transfer coefficients of Zn from root to shoot (Table S3). This is consistent with the observations by Sarret et al.[41] with Zn in *Arabidopsis halleri* grown in solution culture.

Organic acids including citrate, malate, and oxalate are primarily located in the vacuoles[42] and are often found to chelate Zn in leaves [43] and as found by Salt et al.[38] with citrate in shoots of *T. caerulescens*. In

313 the present study, we found that the chemical forms of Zn were similar in all stem and leaf tissues
314 regardless of Zn-treatments, with Zn mainly bound to citrate, histidine, and phytate (Table 1). It is not
315 possible to exclude the presence of other compounds with carboxyl groups (e.g. malate), but our results
316 support the role of carboxyl groups as important ligands involved in the transport and storage of Zn in
317 shoots.[38, 43]
318
319 Surprisingly, there is comparatively little information regarding the speciation of Zn in seeds. The LCF
320 results revealed that ca. 80% of the Zn was coordinated with amino acids such as histidine and cysteine,
321 with a smaller proportion precipitated with phosphate (Table 1). Phytic acid has been found to be the
322 main storage form of P in cereals[44], and that phytate has a high affinity for Zn, Fe, and other trace
323 elements.[45] The co-localization of phytate with these elements[46] seems to support the hypothesis that
324 phytate plays an important role in the storage of Zn in the seeds or grains. However, LCF results in the
325 present study (Table 1) showed that Zn was predominantly associated with amino acids (histidine and
326 cysteine). Indeed, the importance of amino acids (c.f. phytate) for Zn storage has been reported previously
327 in barley (*Hordeum vulgare* L.) grain. For example, Persson et al.[47] incubated barley grain with phytase
328 which degrades phytate, a treatment that doubled the extraction efficiency of P but have no effect on that
329 of Zn. Rather, Zn was found to be bound mainly to peptides as measured using SEC/IP-ICP-MS.
330 Similarly, in a study with low-phytate barley grain mutants, Hatzack et al.[48] found that impaired phytate
331 accumulation did not influence Zn storage capacity in the grains.
332
333 Limitations of the XAS techniques employed in this study include uncertainty in species of ca. 5% of the
334 total amount of the target element [49, 50] which may result in the XAS analysis being insufficiently
335 sensitive to identify small amounts of ZnO-NPs in plants and in soils.
336
337 In summary, we have not detected the translocation of ZnO-NPs from roots to shoots of plants grown in
338 either solution or soil culture, although there was a substantial quantity of ZnO-NPs on the surface of
339 roots exposed to ZnO-NP in solution culture. Even though large quantities of pristine NPs were applied

directly to the soil with which they were mixed thoroughly, the ZnO-NPs appeared to be completely dissociated after 1 h incubation and transformed in similar manner to the $ZnCl_2$ treatment. Indeed, there was no significant difference between the ZnO-NP and $ZnCl_2$ treatments in plant growth, Zn accumulation, or Zn speciation in plant tissues. We conclude, therefore, that under the current experimental conditions, there were no nano-specific effects on plants grown in soil, and that this finding needs to be considered in environmental risk assessment and management strategies.

ASSOCIATED CONTENT

Supporting Information

Additional information is available regarding the characteristics of soils used in this study, cowpea biomass, Zn concentration in various plant tissues, results of the PCA analysis, target transformation SPOIL values of reference spectra, and the Fourier Transform of EXAFS spectra for all soil samples. This material is available free of charge via the Internet at http://pubs.acs.org.

AUTHOR INFORMATION

Corresponding Author

*Email: p.wang3@uq.edu.au; tel: +61 7 3365 4816; fax: +61 7 3365 1177.

Notes

The authors declare no competing financial interest.

ACKNOWLEDGEMENTS

This research was mainly undertaken at the XAS (AS123/XFM/5349) and XFM (AS131/XAS/5723) Beamlines at the Australian Synchrotron, Victoria, Australia. Support was provided to Dr Wang as a recipient of an Australian Research Council (ARC) DECRA (DE130100943) and to Dr Kopittke and Prof Lombi as recipients of ARC Future Fellowships (FT120100277 and FT100100337, respectively). This research was also supported under the ARC Linkage Projects funding scheme (LP130100741).

REFERENCES

1. Ju-Nam, Y.; Lead, J. R., Manufactured nanoparticles: An overview of their chemistry, interactions and potential environmental implications. *Sci. Total Environ.* **2008,** *400* (1-3), 396-414.
2. Milani, N.; McLaughlin, M. J.; Stacey, S. P.; Kirby, J. K.; Hettiarachchi, G. M.; Beak, D. G.; Cornelis, G., Dissolution kinetics of macronutrient fertilizers coated with manufactured zinc oxide nanoparticles. *J. Agr. Food Chem.* **2012,** *60* (16), 3991-3998.
3. Zhu, H.; Han, J.; Xiao, J. Q.; Jin, Y., Uptake, translocation, and accumulation of manufactured iron oxide nanoparticles by pumpkin plants. *J. Environ. Monitor.* **2008,** *10* (6), 713-717.
4. Unrine, J. M.; Shoults-Wilson, W. A.; Zhurbich, O.; Bertsch, P. M.; Tsyusko, O., Trophic transfer of Au nanoparticles from soil along a simulated terrestrial food chain. *Environ. Sci. Technol.* **2012**. *46* (7), 9357-9360.
5. Ma, X.; Geiser-Lee, J.; Deng, Y.; Kolmakov, A., Interactions between engineered nanoparticles (ENPs) and plants: Phytotoxicity, uptake and accumulation. *Sci. Total Environ.* **2010,** *408* (16), 3053-3061.
6. Dietz, K.-J.; Herth, S., Plant nanotoxicology. *Trends Plant Sci.* **2011,** *16* (11), 582-589.
7. Lin, D. H.; Xing, B. S., Root uptake and phytotoxicity of ZnO nanoparticles. *Environ. Sci. Technol.* **2008,** *42* (15), 5580-5585.
8. Du, W.; Sun, Y.; Ji, R.; Zhu, J.; Wu, J.; Guo, H., TiO_2 and ZnO nanoparticles negatively affect wheat growth and soil enzyme activities in agricultural soil. *J. Environ. Monitor.* **2011,** *13* (4), 822-828.
9. Dimkpa, C. O.; Latta, D. E.; McLean, J. E.; Britt, D. W.; Boyanov, M. I.; Anderson, A. J., Fate of CuO and ZnO nano- and microparticles in the plant environment. *Environ. Sci. Technol.* **2013,** *47* (9), 4734-4742.
10. Hernandez-Viezcas, J. A.; Castillo-Michel, H.; Andrews, J. C.; Cotte, M.; Rico, C.; Peralta-Videa, J. R.; Ge, Y.; Priester, J. H.; Holden, P. A.; Gardea-Torresdey, J. L., In situ synchrotron X-ray fluorescence mapping and speciation of CeO_2 and ZnO nanoparticles in soil cultivated soybean (*Glycine max*). *ACS Nano* **2013,** *7* (2), 1415-1423.
11. Birbaum, K.; Brogioli, R.; Schellenberg, M.; Martinoia, E.; Stark, W. J.; Günther, D.; Limbach, L. K., No evidence for cerium dioxide nanoparticle translocation in maize plants. *Environ. Sci. Technol.* **2010,** *44* (22), 8718-8723.
12. Brunner, T. J.; Wick, P.; Manser, P.; Spohn, P.; Grass, R. N.; Limbach, L. K.; Bruinink, A.; Stark, W. J., In vitro cytotoxicity of oxide nanoparticles: Comparison to asbestos, silica, and the effect of particle solubility. *Environ. Sci. Technol.* **2006,** *40* (14), 4374-4381.

13. Lombi, E.; Donner, E.; Tavakkoli, E.; Turney, T.; Naidu, R.; Miller, B. W.; Scheckel, K. G., Fate of zinc oxide nanoparticles during anaerobic digestion of wastewater and post-treatment processing of sewage sludge. *Environ. Sci. Technol.* **2012,** *46* (16), 9089-9096.
14. Scheckel, K. G.; Luxton, T. P.; El Badawy, A. M.; Impellitteri, C. A.; Tolaymat, T. M., Synchrotron speciation of silver and zinc oxide nanoparticles aged in a kaolin suspension. *Environ. Sci. Technol.* **2010,** *44* (4), 1307-1312.
15. Reed, R. B.; Ladner, D. A.; Higgins, C. P.; Westerhoff, P.; Ranville, J. F., Solubility of nano-zinc oxide in environmentally and biologically important matrices. *Environ. Toxicol. Chem.* **2012,** *31* (1), 93-99.
16. Alloway, B.; Graham, R.; Stacey, S., Micronutrient Deficiencies in Australian Field Crops. In *Micronutrient Deficiencies in Global Crop Production*, Alloway, B., Ed. Springer Netherlands: 2008; pp 63-92.
17. Kopittke, P. M.; Blamey, F. P. C.; McKenna, B. A.; Wang, P.; Menzies, N. W., Toxicity of metals to roots of cowpea in relation to their binding strength. *Environ. Toxicol. Chem.* **2011,** *30* (8), 1827-1833.
18. Schwab, A. P., The soil solution. In *Handbook of Soil Science*, Sumner, M. E., Ed. CRC Press: New York, 2000; pp B85-B88.
19. Priester, J. H.; Ge, Y.; Mielke, R. E.; Horst, A. M.; Moritz, S. C.; Espinosa, K.; Gelb, J.; Walker, S. L.; Nisbet, R. M.; An, Y.-J.; Schimel, J. P.; Palmer, R. G.; Hernandez-Viezcas, J. A.; Zhao, L.; Gardea-Torresdey, J. L.; Holden, P. A., Soybean susceptibility to manufactured nanomaterials with evidence for food quality and soil fertility interruption. *Proc. Natl. Acad. Sci. U. S. A.* **2012,** *109* (37), E2451–E2456.
20. Lombi, E.; Nowack, B.; Baun, A.; McGrath, S. P., Evidence for effects of manufactured nanomaterials on crops is inconclusive. *Proc. Natl. Acad. Sci. U. S. A.* **2012,** *109* (49), E3336.
21. Kopittke, P. M.; Menzies, N. W.; de Jonge, M. D.; McKenna, B. A.; Donner, E.; Webb, R. I.; Paterson, D. J.; Howard, D. L.; Ryan, C. G.; Glover, C. J.; Scheckel, K. G.; Lombi, E., In situ distribution and speciation of toxic copper, nickel, and zinc in hydrated roots of cowpea. *Plant Physiol.* **2011,** *156* (2), 663-673.
22. Ravel, B.; Newville, M., ATHENA, ARTEMIS, HEPHAESTUS: data analysis for X-ray absorption spectroscopy using IFEFFIT. *J. Synchrotron Radiat.* **2005,** *12*, 537-541.
23. Malinowski, E. R., *Factor analysis in chemistry*. John Wiley: New York, 1991.
24. Webb, S. M., SIXpack: A graphical user interface for XAS analysis using IFEFFIT. *Physica Scripta* **2005,** *T115*, 1011-1014.
25. Wang, P.; Menzies, N. W.; Lombi, E.; McKenna, B. A.; de Jonge, M. D.; Donner, E.; Blamey, F. P. C.; Ryan, C. G.; Paterson, D. J.; Howard, D. L.; James, S. A.; Kopittke, P. M., Quantitative

435 determination of metal and metalloid spatial distribution in hydrated and fresh roots of cowpea using
436 synchrotron-based X-ray fluorescence microscopy. *Sci. Total Environ.* **2013,** *463–464* (0), 131-139.
437 26. Ryan, C. G.; Etschmann, B. E.; Vogt, S.; Maser, J.; Harland, C. L.; van Achterbergh, E.; Legnini, D.,
438 Nuclear microprobe-synchrotron synergy: Towards integrated quantitative real-time elemental
439 imaging using PIXE and SXRF. *Nucl. Instrum. Meth. B* **2005,** *231*, 183-188.
440 27. Ryan, C. G.; Siddons, D. P.; Kirkham, R.; et al., The mew Maia detector system: Methods for high
441 definition trace element imaging of natural material. In *X-Ray Optics and Microanalysis,*
442 *Proceedings*, Denecke, M. A.; Walker, C. T., Eds. 2010; Vol. 1221, pp 9-17.
443 28. Donner, E.; Howard, D. L.; Jonge, M. D. d.; Paterson, D.; Cheah, M. H.; Naidu, R.; Lombi, E., X-ray
444 absorption and micro X-ray fluorescence spectroscopy investigation of copper and zinc speciation in
445 biosolids. *Environ. Sci. Technol.* **2011,** *45* (17), 7249-7257.
446 29. Hayes, S. M.; O'Day, P. A.; Webb, S. M.; Maier, R. M.; Chorover, J., Changes in zinc speciation
447 with mine tailings acidification in a semiarid weathering environment. *Environ. Sci. Technol.* **2011,**
448 *45* (17), 7166-7172.
449 30. Franklin, N. M.; Rogers, N. J.; Apte, S. C.; Batley, G. E.; Gadd, G. E.; Casey, P. S., Comparative
450 toxicity of nanoparticulate ZnO, bulk ZnO, and $ZnCl_2$ to a freshwater microalga (*Pseudokirchneriella*
451 *subcapitata*): The importance of particle solubility. *Environ. Sci. Technol.* **2007,** *41* (24), 8484-8490.
452 31. Miao, A. J.; Zhang, X. Y.; Luo, Z.; Chen, C. S.; Chin, W. C.; Santschi, P. H.; Quigg, A., Zinc oxide-
453 engineered nanoparticles: dissolution and toxicity to marine phytoplankton. *Environ. Toxicol. Chem.*
454 **2010,** *29* (12), 2814-2822.
455 32. Ma, H.; Williams, P. L.; Diamond, S. A., Ecotoxicity of manufactured ZnO nanoparticles – A review.
456 *Environ. Pollut.* **2013,** *172* (0), 76-85.
457 33. Smolders, E.; Buekers, J.; Waegeneers, N.; Oliver, I.; McLaughlin, M. J. *Effects of field and*
458 *laboratory Zn contamination on soil microbial processes and plant growth*; Katholieke Universiteit
459 Leuven and Commonwealth Scientific and Industrial Research Organisation: Leuven, Belgium, 2003.
460 34. Zhao, L.; Hernandez-Viezcas, J. A.; Peralta-Videa, J. R.; Bandyopadhyay, S.; Peng, B.; Munoz, B.;
461 Keller, A. A.; Gardea-Torresdey, J. L., ZnO nanoparticle fate in soil and zinc bioaccumulation in
462 corn plants (*Zea mays*) influenced by alginate. *Environ. Sci. Proc. Impacts* **2013,** *15* (1), 260-266.
463 35. Waalewijn-Kool, P. L.; Diez Ortiz, M.; van Straalen, N. M.; van Gestel, C. A. M., Sorption,
464 dissolution and pH determine the long-term equilibration and toxicity of coated and uncoated ZnO
465 nanoparticles in soil. *Environ. Pollut.* **2013,** *178* (0), 59-64.
466 36. Collins, D.; Luxton, T.; Kumar, N.; Shah, S.; Walker, V. K.; Shah, V., Assessing the impact of
467 copper and zinc oxide nanoparticles on soil: A field study. *PLoS One* **2012,** *7* (8), e42663.
468 37. Gimbert, L. J.; Hamon, R. E.; Casey, P. S.; Worsfold, P. J., Partitioning and stability of engineered
469 ZnO nanoparticles in soil suspensions using flow field-flow fractionation. *Environ. Chem.* **2007,** *4* (1),
470 8-10.

38. Salt, D. E.; Prince, R. C.; Baker, A. J. M.; Raskin, I.; Pickering, I. J., Zinc ligands in the metal hyperaccumulator *Thlaspi caerulescens* as determined using X-ray absorption spectroscopy. *Environ. Sci. Technol.* **1999,** *33* (5), 713-717.
39. Kupper, H.; Lombi, E.; Zhao, F. J.; McGrath, S. P., Cellular compartmentation of cadmium and zinc in relation to other elements in the hyperaccumulator *Arabidopsis halleri*. *Planta* **2000,** *212* (1), 75-84.
40. Zhao, F. J.; Lombi, E.; Breedon, T.; McGrath, S. P., Zinc hyperaccumulation and cellular distribution in *Arabidopsis halleri*. *Plant Cell Environ.* **2000,** *23* (5), 507-514.
41. Sarret, G.; Saumitou-Laprade, P.; Bert, V.; Proux, O.; Hazemann, J. L.; Traverse, A. S.; Marcus, M. A.; Manceau, A., Forms of zinc accumulated in the hyperaccumulator *Arabidopsis halleri*. *Plant Physiol.* **2002,** *130* (4), 1815-1826.
42. Ryan, C. A.; Walkersimmons, M., Plant vacuoles. *Methods in Enzymology* **1983,** *96*, 580-589.
43. Sarret, G.; Willems, G.; Isaure, M. P.; Marcus, M. A.; Fakra, S. C.; Frerot, H.; Pairis, S.; Geoffroy, N.; Manceau, A.; Saumitou-Laprade, P., Zinc distribution and speciation in *Arabidopsis halleri* x *Arabidopsis lyrata* progenies presenting various zinc accumulation capacities. *New Phytol.* **2009,** *184* (3), 581-595.
44. Raboy, V., myo-Inositol-1,2,3,4,5,6-hexakisphosphate. *Phytochemistry* **2003,** *64* (6), 1033-1043.
45. Vasca, E.; Materazzi, S.; Caruso, T.; Milano, O.; Fontanella, C.; Manfredi, C., Complex formation between phytic acid and divalent metal ions: a solution equilibria and solid state investigation. *Anal. Bioanal. Chem.* **2002,** *374* (1), 173-178.
46. Mills, E. N. C.; Parker, M. L.; Wellner, N.; Toole, G.; Feeney, K.; Shewry, P. R., Chemical imaging: the distribution of ions and molecules in developing and mature wheat grain. *J. Cereal Sci.* **2005,** *41* (2), 193-201.
47. Persson, D. P.; Hansen, T. H.; Laursen, K. H.; Schjoerring, J. K.; Husted, S., Simultaneous iron, zinc, sulfur and phosphorus speciation analysis of barley grain tissues using SEC-ICP-MS and IP-ICP-MS. *Metallomics* **2009,** *1* (5), 418-426.
48. Hatzack, F.; Johansen, K. S.; Rasmussen, S. K., Nutritionally relevant parameters in low-phytate barley (*Hordeum vulgare* L.) grain mutants. *J. Agr. Food Chem.* **2000,** *48* (12), 6074-6080.
49. Kirpichtchikova, T. A.; Manceau, A.; Spadini, L.; Panfili, F.; MarcuS, M. A.; Jacquet, T., Speciation and solubility of heavy metals in contaminated soil using X-ray microfluorescence, EXAFS spectroscopy, chemical extraction, and thermodynamic modeling. *Geochim. Cosmochim. Ac.* **2006,** *70* (9), 2163-2190.
50. Manceau, A.; Marcus, M. A.; Tamura, N., Quantitative speciation of heavy metals in soils and sediments by synchrotron X-ray techniques. *Rev. Mineral. Geochem.* **2002,** *49* (1), 341-428.

Table 1. Distributions of Zn species in various tissues of cowpea grown in either solution culture or soil culture[a]

	Nodule		Root		Stem		Leaf		Seed	
	ZnO-NP	$ZnCl_2$	ZnO-NP	$ZnCl_2$	ZnO-NP	$ZnCl_2$	ZnO-NP	$ZnCl_2$	ZnO-NP	$ZnCl_2$
Solution culture										
ZnO-NPs (%)			65 (1.1)							
Zn-PGA (%)[c]				32 (0.7)						
Zn-citrate (%)					76 (0.6)	63 (1.0)	60 (1.2)	75 (1.0)		
Zn-histidine (%)			32 (0.9)	49 (1.7)	14 (1.0)	17 (1.5)	25 (1.9)	10 (1.5)		
Zn-phytate (%)					10 (1.2)	20 (2.0)	15 (2.4)	15 (1.9)		
Zn-cysteine (%)										
Zn-phosphate (%)			3 (0.7)	19 (3.0)						
R-factor[b]			0.0001	0.0002	0.0001	0.0003	0.0005	0.0003		
Soil culture										
Zn-citrate (%)	42 (1.5)	31 (1.2)	59 (0.8)	43 (0.8)	27 (1.1)	34 (1.9)	50 (0.9)	41 (0.7)		
Zn-histidine (%)			25 (1.2)	30 (1.2)	38 (1.6)	34 (2.9)	43 (1.4)	27 (1.1)	56 (1.3)	45 (1.4)
Zn-phytate (%)	38 (2.1)	37 (1.4)	16 (1.4)	27 (1.5)	35 (2.1)	32 (3.6)	7 (1.8)	32 (1.4)		
Zn-cysteine (%)	22 (0.9)	32 (0.7)							24 (1.1)	36 (1.1)
Zn-phosphate (%)									20 (1.7)	19 (1.8)
R-factor[b]	0.0006	0.0003	0.0002	0.0002	0.0004	0.0005	0.0003	0.0002	0.0003	0.0004

[a]Data are presented as percentages and the values in brackets show the percentage variation in the calculated values. [b]R factor = $\sum(\text{experimental} - \text{fit})^2 / \sum(\text{experimental})^2$, where the sums are over the data points in the fitting region. [c]PGA: polygalacturonic acid.

Table 2. Best fit speciation of Zn in soils as identified by linear combination fitting (LCF) of K_α-edge XANES and EXAFS spectra[a]

	XANES					EXAFS			
	ZnAl-LDH	Zn-sorb ferr.[c]		$ZnSO_4$	R-factor[b]	ZnAl-LDH	hemimorphite	$ZnSO_4$	R-factor[b]
Oxisol									
ZnO-NPs 1h	30 (1.0)	45 (0.6)		25 (1.2)	0.0003	38 (5.2)	44 (1.6)	18 (5.5)	0.057
ZnO-NPs 1d	24 (1.1)	44 (0.6)		32 (1.2)	0.0003	26 (5.4)	48 (1.6)	26 (5.6)	0.063
ZnO-NPs 5d	28 (1.1)	41 (0.6)		31 (1.3)	0.0004	36 (5.1)	41 (1.5)	23 (5.3)	0.057
ZnO-NPs 15d	24 (1.2)	43 (0.7)		33 (1.4)	0.0004	27 (5.4)	45 (1.7)	28 (5.7)	0.066
$ZnCl_2$ 1 h	23 (1.5)	55 (0.8)		22 (1.7)	0.0007	24 (5.5)	47 (1.7)	29 (5.7)	0.081
$ZnCl_2$ 1 d	22 (1.4)	53 (0.8)		25 (1.6)	0.0005	29 (5.7)	47 (1.7)	24 (5.9)	0.082
$ZnCl_2$ 5 d	21 (1.6)	55 (0.9)		24 (1.8)	0.0004	22 (6.9)	53 (2.1)	25 (7.2)	0.096
$ZnCl_2$ 15 d	22 (1.4)	54 (0.8)		24 (1.6)	0.0006	22 (5.9)	45 (1.8)	33 (6.1)	0.088
	ZnAl-LDH	HA-Zn	hopeite	$ZnSO_4$					
Ultisol									
ZnO-NPs 1h	15 (0.7)	29 (1.8)	17 (1.4)	40 (2.3)	0.0001	31 (6.5)	36 (2.0)	33 (6.7)	0.079
ZnO-NPs 1d	16 (0.8)	27 (1.8)	16 (1.4)	41 (2.4)	0.0001	31 (6.3)	35 (1.9)	34 (6.6)	0.076
ZnO-NPs 5d	12 (0.9)	27 (2.2)	15 (1.7)	46 (2.9)	0.0002	36 (5.1)	41 (1.5)	23 (5.3)	0.058
ZnO-NPs 15d	9 (0.9)	28 (2.2)	15 (1.7)	49 (2.9)	0.0002	27 (5.4)	45 (1.7)	28 (5.7)	0.066
$ZnCl_2$ 1 h	10 (0.9)	21 (2.1)	19 (1.7)	50 (2.9)	0.0002	26 (7.5)	32 (2.3)	42 (7.8)	0.097
$ZnCl_2$ 1 d	13 (1.1)	10 (0.8)	26 (2.0)	51 (3.5)	0.0002	18 (6.5)	35 (2.0)	47 (6.8)	0.080
$ZnCl_2$ 5 d	16 (1.1)	24 (2.4)	50 (1.9)	10 (3.3)	0.0002	34 (7.2)	46 (2.2)	20 (7.6)	0.109
$ZnCl_2$ 15 d	16 (1.2)	27 (2.6)	47 (2.0)	10 (3.5)	0.0003	32 (8.4)	45 (2.6)	23 (8.8)	0.140

[a]Data are presented as percentages and the values in brackets show the percentage variation in the calculated values. [b]R factor = $\sum(\text{experimental} - \text{fit})^2 / \sum(\text{experimental})^2$, where the sums are over the data points in the fitting region. [c]Zn sorbed ferrihydrite.

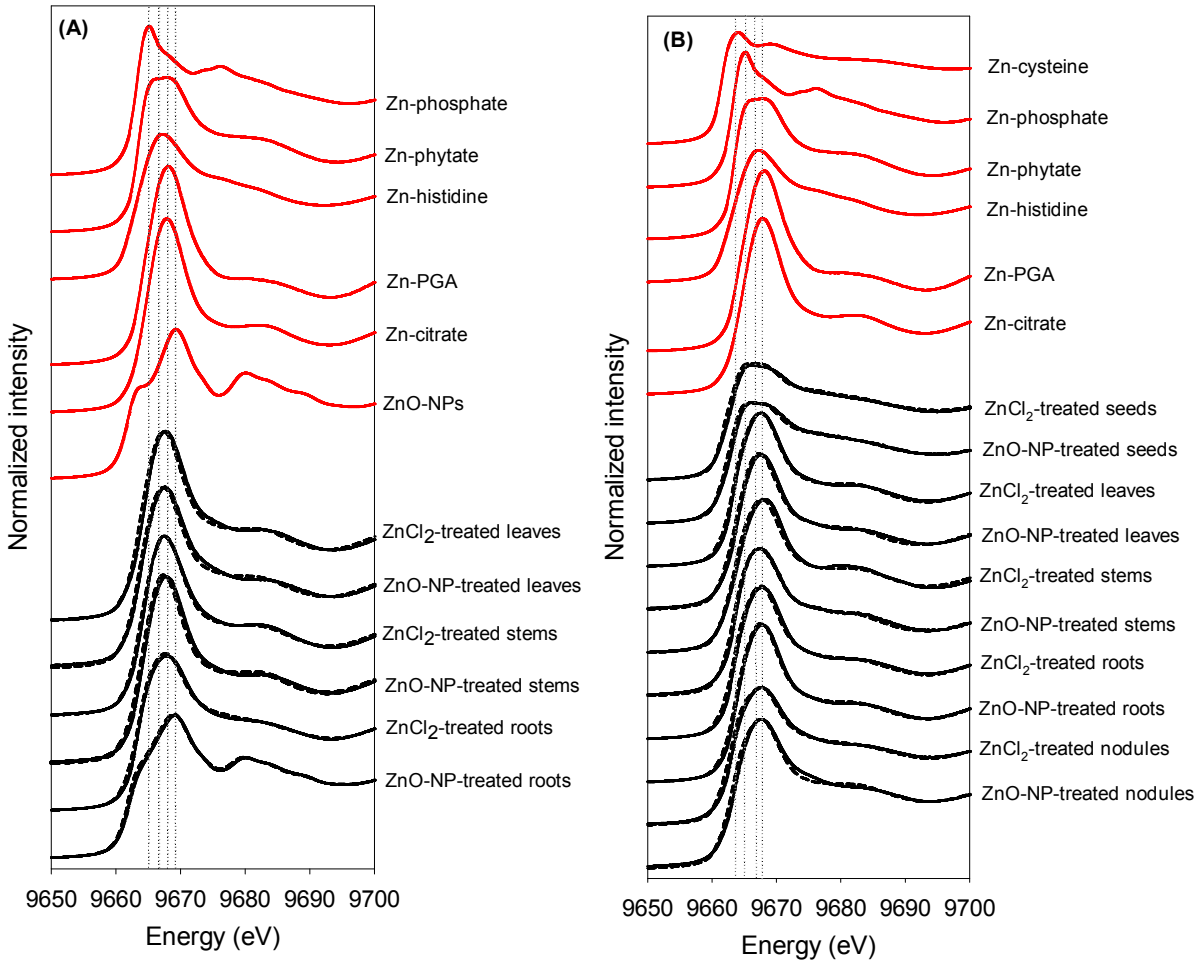

Figure 1. Normalized Zn K_α-edge XANES spectra for various tissues of cowpea exposed to ZnO-NPs or $ZnCl_2$ in solution culture (A) or soil culture (B). Data are also presented for the standard compounds determined in the LCF solutions. Dotted lines show the best fits of reference spectra obtained using LCF as presented in Table 1.

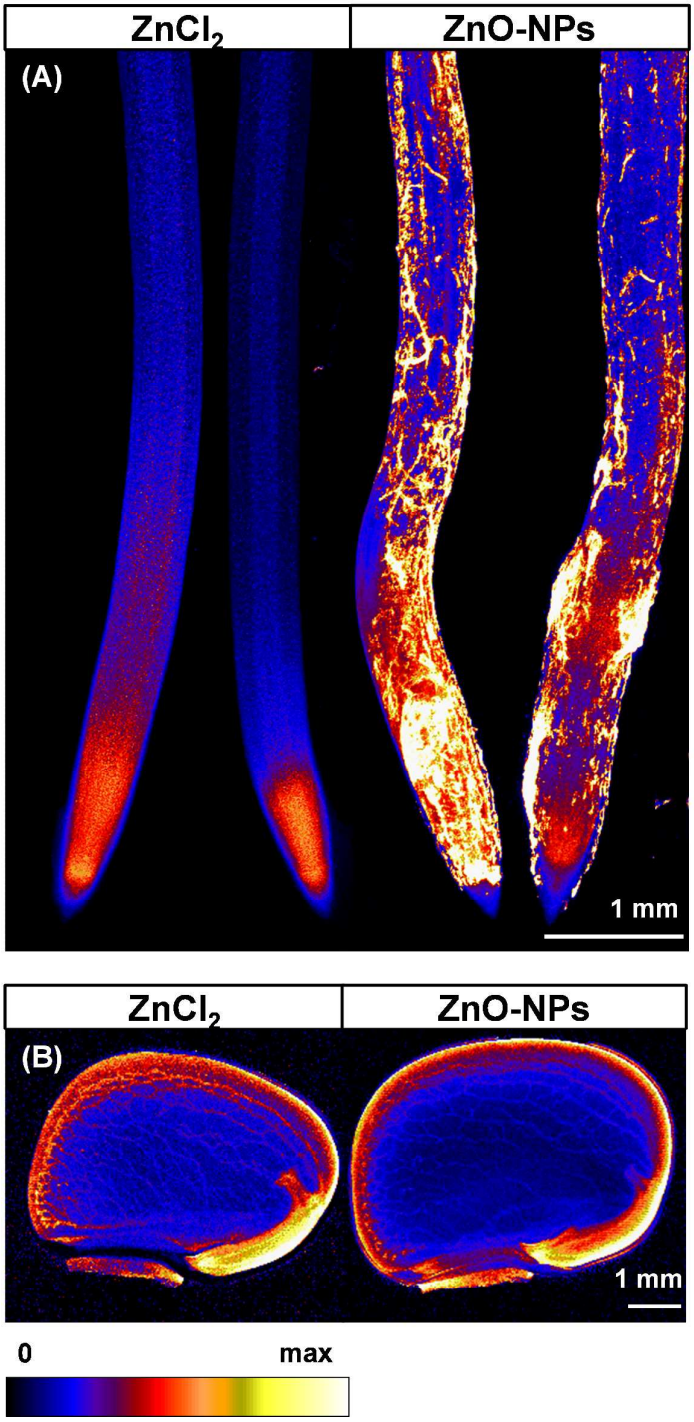

Figure 2. (A) Imaging of Zn in cowpea roots exposed for 1 d to 25 mg Zn L^{-1} as ZnO-NPs or $ZnCl_2$ in solution culture using μ-XRF. (B) Imaging of Zn in cowpea seeds grown in the Oxisol amended with $ZnCl_2$ or ZnO-NPs using μ-XRF. All samples were enclosed in 4 μm-thick Ultralene films and scanned simultaneously allowing valid comparisons between treatments. Brighter colors correspond to higher Zn concentrations.

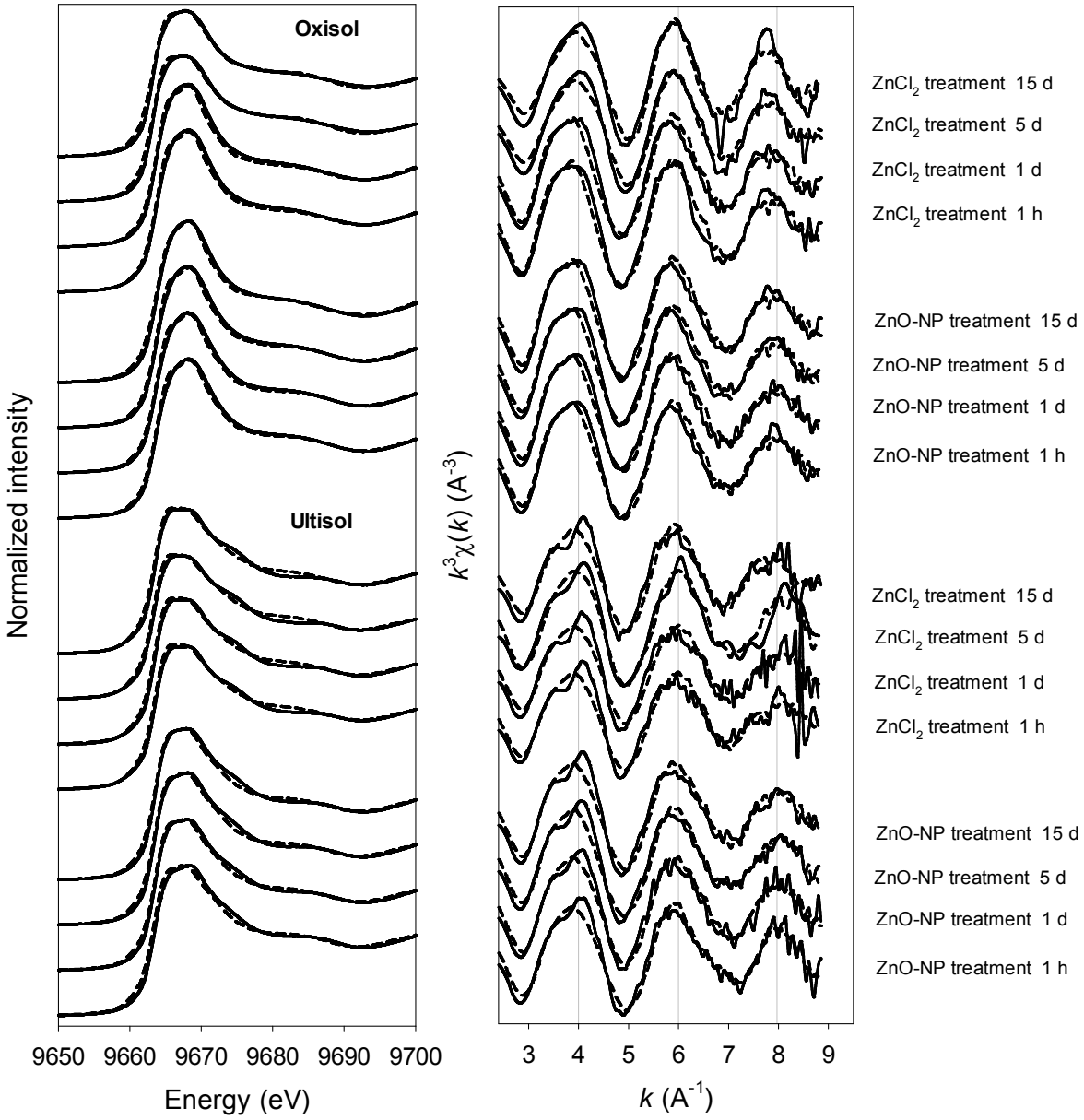

Figure 3. Zn K_α-edge XANES and k^3-weighted EXAFS spectra of two soils (Oxisol and Ultisol) amended with 500 mg Zn kg^{-1} as $ZnCl_2$ or ZnO-NPs incubated for 1 h, 1 d, 5 d, and 15 d. Dotted lines show the best fits of reference spectra obtained using LCF as presented in Table 2.

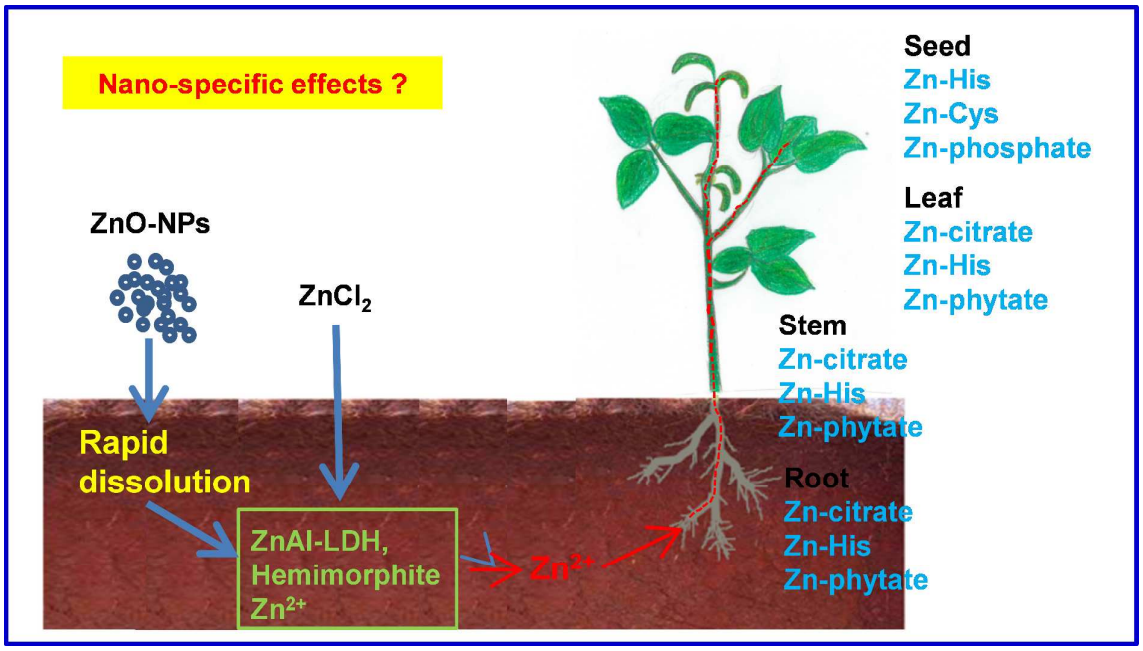

TOC Graphic Image